'A forz 'e l'ambizione è chell c'avvicin 'e stell a terr

"The power of ambition is what brings the stars closer to the ground"

- Co'Sang

Abstract

perché

Acknowledgments

Thanksss

Contents

List of Figures

List of Tables

List of Abbreviations and Acronyms

AFSPC	Air Force Space Command
API	Application Programming interface
BC	Ballistic Coefficient
COESA	Committee On Extension to the Standard Atmosphere
DMU	Drag Make Up
DRAMA	Debris Risk Assessment and Mitigation Analysis
ECEF	Earth-Centered Earth-Fixed
ECI	Earth-Centered Inertia
GEO	Geostationary Orbit
GMAT	General Mission Analysis Tool
IAM	Inclination Adjust Maneuvers
JB2008	Jacchia-Bowman 2008
JIT	Just-In-Time
LEO	Low Earth Orbit

MIT	Massachusetts Institute of Technology
MLTAN	Mean Local Time of the Ascending Node
NASA	National Aeronautics and Space Administration
RAAN	Right Ascension of the Ascending Node
SRP	Solar-Radiation Pressure
SSO	Sun-Synchronous Orbit
TLE	Two-Line Element
UTC	Coordinate Universal Time

Chapter 1

Introduction

1.1 Earth Observation and Remote Sensing

1.1.1 Hyperspectral imaging

1.2 Kuva Space

1.2.1 Company Vision

1.2.2 Infrastructure

1.2.3 Distribution

1.2.4 Applications

1.3 Thesis Purpose

1.4 Organization

Chapter 2

Background

This chapter aims to provide an overview on the fundamentals of Space Flight Dynamics that constitute the theoretical basis of this thesis, with a specific focus on Earth Observation applications in Low Earth Orbit (LEO), as well as a literature review on orbit management methods addressed by this work.

2.1 Space Flight Dynamics Introduction

Orbital Mechanics, Astrodynamics, Astronautics and Space Flight Dynamics are all titles of university courses whose principal topic is two-body orbital motion, that involves orbit determination, orbital flight time, and orbital maneuvers [5]. In this context, a proper definition of the subject can be the following: the study of the motion of man-made objects in space, subject to both natural and artificially induced forces [6].

2.1.1 Satellite State Representations

To define the *state* of a satellite in space six quantities are required, and they may take on many equivalent forms. Whatever the form, the collection is called either a *state vector*, usually associated with position and velocity vectors, or an *element*

set, typically used with scalar magnitude and angular representations of the orbit called *orbital elements*. Either set of quantities completely specify the two-body orbit and provide a complete set of initial conditions for solving an initial value problem class of differential equations. Time is always associated with a state vector and is often considered a seventh component. State vectors and element sets are referenced to a particular coordinate frame [7].

This thesis will use both state vectors and a specific element set. The latter, which is also the most common one in this field, is represented by the ***classical orbital elements*** [1]:

- Semimajor axis, a: the orbit size is defined by one half of the major axis dimension
- Eccentricity, e: the ratio of minor to major dimensions of an orbit defines the shape
- Inclination, i: the angle between the orbit plane and the reference plane or the angle between the normals to the two planes
- Longitude of the ascending node or Right Ascension of the Ascending Node (RAAN), Ω: the angle between the vernal equinox vector and the ascending node measured in the reference plane in a couterclockwise direction as viewed from the northern hemisphere
- Argument of periapsis, ω: the angle from the ascending node to the periapsis, measured in the orbital plane in the direction of spacecraft motion. The ascending node is the point where the spacecraft crosses the reference plane headed from south to north. the line of nodes is the line formed by the intersection of the orbit plane and the reference plane
- True anomaly, ν: the sixth element locates the spacecraft position on the orbit

This thesis work makes also use of the *argument of latitude, u*, which is the

angle measured between the ascending node and the satellite's position vector in the direction of satellite motion. A relation that is always valid exists between classical orbital elements and the argument of latitude [7]:

$$u = \omega + \nu \tag{2.1}$$

One more element that is often used is the *mean anomaly, M*, which is the angle between the periapsis of an orbit and the position of an imaginary body that orbits in the same period as the real one but at a constant angular speed (circular orbit). The angular speed assigned to the imaginary body is the satellite's average angular velocity over one orbit, and is called *mean motion, n* [8].

This research utilizes also another element set which results necessary to address case studies of past missions: the *Two-line element set* (TLE). A two-line element consists of a satellite identifier, an epoch, six orbital elements and a B^* term related to the ballistic coefficient [9]. These elsets are available to the general public through Air Force Space Command (AFSPC) [7].

The elements of a TLE are shown in equation 2.2 [7], where:

- the bars on the mean motion and semimajor axis denote *Kozai mean values*
- the numerators of the first two elements of the second line represent mean motion rate and acceleration
- $\frac{c_D A}{m}$ corresponds to the inverse of the *ballistic coefficient, BC*
- ρ_0 is the atmospheric density at perigee of the orbit
- $R_\oplus$ defines an Earth Radius of 6378.135 km
- the epoch is expressed in Coordinate Universal Time (UTC)

$$\begin{array}{ccccccc} \bar{n} = \sqrt{\frac{\mu}{\bar{a}^3}} & & e & & i & \Omega & \omega & M \\ \frac{\dot{n}}{2} & & \frac{\ddot{n}}{6} & & B^* = \frac{1}{2}\frac{c_D A}{m}\rho_0 R_\oplus & & UTC & \end{array} \tag{2.2}$$

2.1.2 Reference Frames

Two types of reference frames are adopted by this research: the geocentric-inertial coordinate system and the geographic-body-fixed system. The origin of both systems is the center of mass of the central body, which in all case studies of this work is the Earth. They will therefore be labeled Earth-centered inertial (ECI) and Eart-centered Earth-fixed (ECEF) coordinate frames, respectively.

Earth-centered inertial

The ECI system is shown in FIGURE???. The equatorial plane is the reference plane. The X axis is the vernal equinox vector, and the Z axis is the spin axis of the Earth; north is positive. The axes are fixed in inertial space or fixed with respect to the stars [1].

Earth-centered Earth-fixed

FIGURE shows a representation of the ECEF reference frame. The system is Earth-centered and fixed to the rotating Earth [7]. Considering the ECI, the Z axis is the same, while the X axis always points towards the Greenwich meridian. Satellite ground track is commonly plotted in this coordinate system [1].

2.1.3 Orbital Perturbations

Orbital perturbations are deviations from a normal, idealized, or undisturbed motion. Introducing an alteration from two-body problem assumptions, the actual motion will vary due to perturbations caused by other bodies, and additional forces not considered in Keplerian motion [7]. This subsection provides an overview of the main perturbations for an Earth orbiting spacecraft.

Earth's Gravity Field

Spinning celestial bodies are nor perfect spheres, but they are much more similar to oblate spheroids. For such a planet, the spin axis can be considered as the axis of rotational symmetry and the gravitational field will vary with the latitude as well as radius. The planet's oblateness provides a rotationally symmetric perturbation Φ, which does not depend on the longitude [2].

In particular, Φ is given by an infinite series characterized by the so-called *zonal harmonics* J_k of the planet of reference. Considering a spherical coordinate system for convenience, with origin at the planet's center of mass and third axis as the axis of rotational symmetry, in this series, shown in equation 2.3, r and ϕ are the distance from the origin and the polar angle respectively, μ is the Earth's standard gravitational parameter, R the equatorial radius and P_k represent the Legendre polynomials [2].

$$\Phi(r, \phi) = \frac{\mu}{r} \sum_{k=2}^{\infty} J_k \left(\frac{R}{r}\right)^k P_k(\cos\phi) \tag{2.3}$$

The zonal harmonics are non-dimensional quantities which are evaluated from satellite observation mission around the planet. The summation starts from $k = 2$, and the Earth's set of zonal harmonics is highly dominated by J_2. Taking into account only J_2 and starting from equation 2.3, it is possible to derivate the perturbing gravitational acceleration due to the respective zonal harmonic [2]:

$$\vec{a}_{J_2} = \frac{3}{2} \frac{J_2 \mu R^2}{r^4} \left[\frac{x}{r} \left(5\frac{z^2}{r^2} - 1\right) \hat{\mathbf{i}} + \frac{y}{r} \left(5\frac{z^2}{r^2} - 1\right) \hat{\mathbf{j}} + \frac{z}{r} \left(5\frac{z^2}{r^2} - 3\right) \hat{\mathbf{k}} \right] \tag{2.4}$$

The right ascension Ω and the argument of perigee ω are significantly affected by oblateness [2].

It is necessary to underline that the Earth's gravitational field vary not only with latitude but also with longitude due to irregularities in geometry and mass

distribution [2]. However, with negligible approximation, it is definitely reasonable to consider only oblateness with J_2 effects in LEO missions, which is the major force for this range of altitudes, second only to Earth's gravity [1]. In light of the above, this thesis will take into account only J_2 forces with respect to the Earth's gravity field perturbations.

Atmospheric Drag

The residual atmosphere present at a few hundred kilometers of altitude strongly influences the motion of satellites in LEO. The basic equation of the perturbing specific force (force per unit mass) due to drag is the following [7]:

$$\vec{a}_{drag} = -\frac{1}{2}\frac{C_D A}{m}\rho V_{rel}^2 \frac{\vec{V_{rel}}}{|\vec{V_{rel}}|} \tag{2.5}$$

In equation 2.5, $\frac{m}{C_D A}$ is again the ballistic coefficient, that already appeared in the TLE representation (equation 2.2): m is the mass of the spacecraft, A represents the cross-sectional area of the satellite with respect to the atmosphere and C_D is the drag coefficient, a dimensionless parameter which takes into account every aerodynamic configuration aspect of the body with respect to the drag forces [10]. The value of the drag coefficient for satellites in the upper atmosphere is generally around 2.2 [7]; this number has been considered for all the case studies of the thesis. Finally, the velocity vector $\vec{V_{rel}}$ is relative to the atmosphere, as well as the cross section.

The main effects provided by aerodynamic drag are changes in the semimajor axis and eccentricity of the orbit and an accurate description of the atmospheric properties is crucial for the evaluation of drag on satellites [7]. However, uncertainties in the time variance of upper atmosphere make perfect prediction of spacecraft drag impossible [1]. More in depth, the density changes because of a complex interaction between three factors: the nature of the atmosphere's

molecular structure, the incident solar flux, and geomagnetic interactions. Several atmospheric models can be found in literature, either static or time-varying. The static ones are less accurate, but definitely simpler than the time-varying models, thanks to the assumption of all constant parameters [7]. This thesis exploits three different models, depending on the applications addressed in the case studies.

The first model considered by this research is static: the exponential model, valid in the range of altitudes between 0 and 1000 km. It assumes a spherically symmetrical distribution of particles of the atmosphere, in which the density decreases exponentially with increasing the altitude according to equation 2.6 [7]

$$\rho = \rho_0 \exp\left[-\frac{h - h_0}{H}\right] \tag{2.6}$$

where ρ_0 and h_0 represent a reference density and altitude respectively and H is the scale height.

The second atmospheric model, still static, is the Standard Atmosphere published in 1976 by the U.S. Committee on Extension to the Standard Atmosphere (COESA), valid drom 0 to 1000 km of altitude. It is an ideal, steady-state model of the Earth's atmosphere at a latitude of 45°N in moderate solar activity conditions [7].

Finally, Jacchia-Bowman 2008 (JB2008) is an empirical time-varying atmospheric density model. It revises and improves the earlier Jacchia-Bowman 2006 which is based on the diffusion equations of the Jacchia 71 model. JB2008 takes into account factors like solar irradiances, computed from driving solar indices based on orbit-based sensor data. Density variations are described by semiannual density equations based on 81-day average solar indices, as well as from temperature equations that include corrections for diurnal and latitudinal effects. Geomagnetic effects are modeled too. The model is validated in the altitude range of 175 to 1000 km through comparisons with accurate daily density drag data pre-

viously collected for numerous satellites, existing atmospheric models and other measurements from several Earth orbiting satellite missions [11, 12].

Third-Body Perturbations

All the orbital elements are periodically affected by the gravitational forces of the Sun and the Moon. Similarly to what is triggered by the Earth's equatorial bulge, they apply an external torque to the orbits and cause the angular momentum to rotate. This perturbation is highly negligible in LEO, where the main effects are provided by J_2 and aerodynamic drag [3]. However, low Earth orbits characterized by a constant geometry with respect to the perturbing body can be affected by emphasized long-period effects. This is the case of Sun-synchronous orbits (SSO), for which the constant pattern with the Sun causes a long-term phenomenon of variation of the inclination (around 0.05 degrees per year) [13]. Although this number might appear meaningless, inclination is critical to SSO, as will be explained in paragraph 2.2.1.

Solar-Radiation Pressure

The last perturbation treated by this thesis is the solar-radiation pressure (SRP), which induces periodic variations in all the orbital elements. SRP generally becomes significant above 800 km of altitude, as drag becomes less important. Below this threshold, it might be neglected [3]. The perturbing acceleration can be approximated by the following equation [7]

$$\vec{a}_{SRP} = -\frac{p_{SRP} c_R A_{\odot}}{m_{sat}} \frac{\vec{r}_{\oplus\odot}}{|\vec{r}_{\oplus\odot}|} \tag{2.7}$$

p_{SRP} is the solar pressure, which is a quantity representing the change in momentum per unit area, derived by the ratio between the solar flux and the speed of light. The reflectivity, c_R, a value between 0.0 and 2.0, models the type of inter-

action between radiation and surface exposed to the Sun, $A_{\odot}$ [7]. m_{sat} is trivially the mass of the satellite.

2.1.4 Mean Orbital Elements

The previous subsection has described how orbital perturbations generate continuous variations and oscillations in the orbit elements. The values of the elements at a single point in time, which are periodically and secularly affected by the perturbing forces, are called *osculating elements*. On the other side, it is possible to define the *mean orbit elements*, which represent the average motion over a span of time [3]. In this way it is possible to obtain a representation of the orbital motion removing short and long-periodic effects induced by perturbations. And for most operational purposes, conversion from osculating to mean elements is indispensable [14]. Indeed, applications addressed by this work, like station-keeping and differential drag, require the secular behavior of the satellite to be implemented.

The oblateness of the Earth is the main guilty of periodic effects, provoking variations in all osculating elements, as well as all the other zonal harmonics. On the other hand, only even zonal gravitational harmonics and atmospheric drag give raise to secular effects in osculating elements, which are constant or non-periodic. Aerodynamic drag secular perturbation plays a crucial role in LEO [15].

Figure 2.1 shows the comparison between osculating and mean semi-major axis of a LEO satellite motion over the course of four months. The orbital decay induced by the atmospheric drag secular effect is evident, as well as the periodic consequences of J_2 perturbation.

Semi-Major Axis

Figure 2.1: Osculating vs. mean semi-major axis for a LEO satellite under atmospheric drag and J_2 perturbations.

Several perturbation techniques have been proposed to perform the conversion

between osculating and mean elements. Brouwer and Kozai works were ones of the first methods appeared in literature, both consisting of first order solutions which take into account the Earth's asphericity but neglect drag effects [16]. This thesis uses a refinement of Brouwer's approach, suggested by Lyddane, which solves zero eccentricity and inclination singularities that are involved in the original theory. Moreover, the algorithm will account only first order J_2 terms [17].

2.1.5 Orbit Propagation

Orbit propagation is the principal problem in perturbation analysis. There are numerous methods to analyse the perturbing force models, and they can be classified in three categories [7]:

- *Special perturbation techniques*: they are numerical solutions, and they represent the most accurate way.
- *General perturbation techniques*: they are analytical methods based on approximations, which means the accuracy is lower, but the computation is speeded up.
- *Semianalytical techniques*: these techniques combine the best features of the previous categories, which means both good accuracy and computational efficiency.

The technique selected to design the tools shown in chapter 4 falls into the first category. Actually, the purposes of the thesis would even be achieved by a general perturbation method, saving time in the calculation phase. Indeed, there are not strict requirements of accuracy, since the research look of this work. However, a special perturbation technique has been chosen in order to provide more valuable tools which might be useful in the advanced stages of future Kuva Space missions. Furthermore, this is also a reasonable choice due to the long-time propagations needed by operations that will be discussed later.

Cowell's Technique

The Cowell's special perturbation technique is implemented in the algorithms produced by this thesis. The idea of this method is to add the perturbing accelerations to the two-body equation:

$$\ddot{\vec{r}} = -\frac{\mu}{r^3}\vec{r} + \vec{a}_p \tag{2.8}$$

$\vec{a}_p$ represents the total acceleration given by the perturbing forces, like that ones seen in paragraph 2.1.3 (e.g., equation 2.5), while $\vec{r}$ is clearly the state vector of the satellite. Equation 2.8 is called *Cowell's formulation* [7].

2.2 Specialized Orbits

Specialized orbits are the results of specific orbital features selected during the design of a mission, which can be simply related to the orbit period or, more commonly, to one of the main orbit perturbations [3]. In this section, two special Earth orbits will be analysed, both of interest for the purposes of the thesis. Ïn fact, in general methods, the higher the propagation times, the lower the accuracy.

2.2.1 Sun-Synchronous Orbit

Sun-synchronous orbits are specialized orbits characterized by a constant geometry with the Sun over time [7]. They are used for several reasons, from technical needs like that ones deriving from thermal and electric power subsystems of the spacecraft to application requirements such as remote sensing. Indeed, a constant Sun angle is very precious for missions working with electro-optical sensors [1]. This is the case, for instance, of hyperspectral technology.

An SSO can be obtained by matching the Westward motion of the line of nodes (*regression of the nodes*) to the solar motion projected on the equator, like shown

in equation 2.9 [1].

$$\dot{\Omega} = 360°/365.242\ days = 0.9856\ °/day \tag{2.9}$$

This will allow the satellite's line of nodes to keep a constant angular separation with respect to the Sun. This separation can be achieved with very good approximation only considering the dominant cause of the secular motion of RAAN: J_2 perturbation. The secular behavior of Ω induced by the oblateness is function of semi-major axis, eccentricity and inclination and is given by the following formula [7]:

$$\dot{\Omega}(a, e, i) = -\frac{3nR_{\oplus}^2 J_2}{2a^2(1-e^2)^2}\cos i \tag{2.10}$$

Equations 2.9 and 2.10 suggest that to achieve the proper $\dot{\Omega}$ of an SSO, the inclination has to be more than 90° (*retrograde orbit*), so that the term $\cos i$ will become negative [3]. As for the other two variables, eccentricity is generally supposed to be near-zero because low-Earth orbits usually imply very small values of e. Hence, with the assumption of $e = 0$, an SSO will be characterized by a direct relationship between a and i. Figure 2.2 shows the range of inclinations and altitudes that would provide the proper regression of nodes.

In addition, it is possible to select the initial value of the RAAN between 0 and 360 degrees according to the mission requirements for example [7]. The angle between the ascending node and the direction of the Sun is commonly labeled like *Mean Local Time of the Ascending Node* (MLTAN), because of the relative time to the noon meridian. This is a crucial design parameter because, while for an arbitrary orbit the MLTAN would continually change, for a Sun-synchronous orbit it will remain constant [18] (not only at the nodes, but at any latitude).

In order to provide a better understanding of the concepts, figure 2.3 shows an example of an SSO with an LTAN of 15:00.

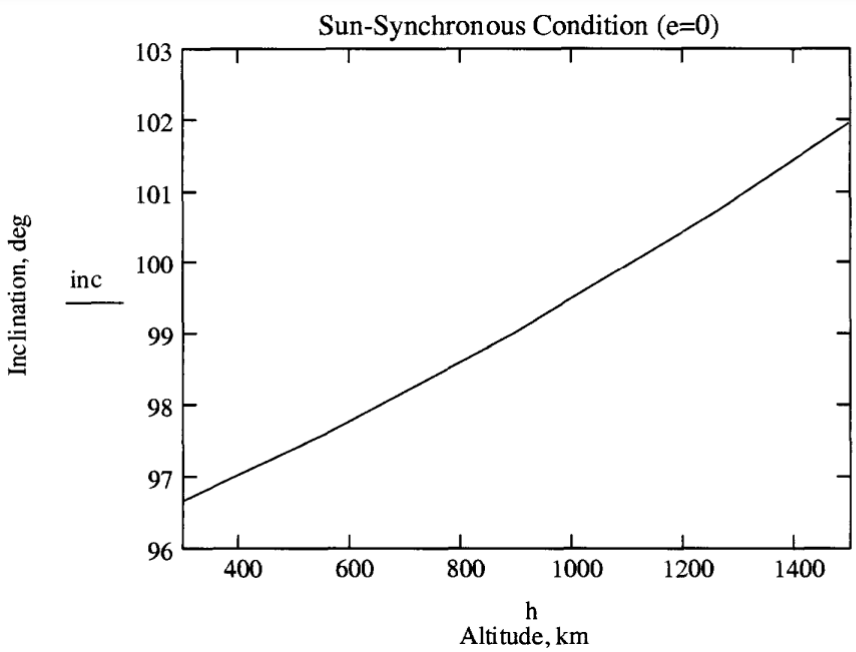

Figure 2.2: SSO condition: inclination vs. altitude ($e = 0$) [1].

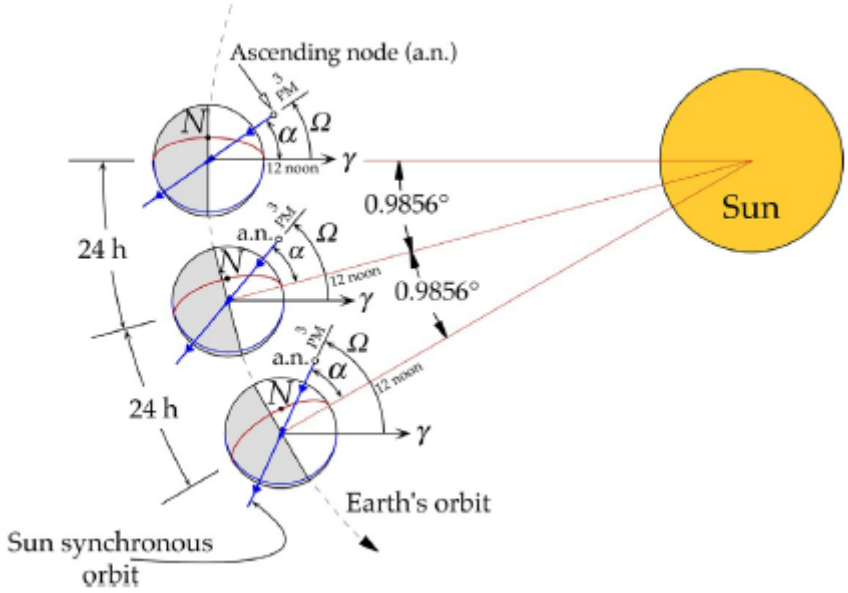

Figure 2.3: Sun-synchronous orbit 15:00 LTAN illustration [2].

2.2.2 Repeat-Groundtrack Orbit

The peculiarity of a *repeat-groundtrak orbit* is the repetitive transit of the satellite to the same location relative to the surface of the Earth after a certain time interval [3]. Hence, they are used by missions which need to periodically revisit a specific point on the Earth [7], playing an interesting role in remote sensing applications.

Considering j orbit periods and the relative k days spent, an orbit is repetitive if and only if the ratio Q between j and k is a rational number, where Q represents the number of orbits per day. This means that j and k are integer and prime to each other. For instance, if a satellite performs 15.25 orbits per day, it will make a 4-day repeating ground track, because the respective rational Q is given by $j = 61$ orbits in $k = 4$ days [3]. k is typically known as the *revisit time* of the spacecraft, defined as the time elapsed between two successive observations of the same ground point [19]. It is necessary to underline that the effects of perturbations should be taken into account in order to obtain accurate repetition properties, since the actual period appears more complex [3].

In light of the above, it can be easily understood that the minimum achievable revisit time for a generic orbit is 1 day. However, mission objectives might require shorter revisit times. The solution to this issue is the design of a constellation of satellites, as will be discussed later.

2.3 Satellite Constellations

A satellite constellation can be defined as a group of similar satellites, with comparable functions and properties, designed to operate in similar, complementary orbits to undertake common objectives, under shared control [20]. In the context of this thesis, constellations are of notable interest thanks to the wide coverage of the world they can enhance with respect to a single satellite mission. Applications like communication, navigation and surveillance drastically improve their service

performances and extend market opportunities when considering a constellation infrastructure.

2.3.1 Walker Delta Constellation

Walker constellations are the most symmetric of the satellite pattern families. The *Walker Delta* is the most popular model within the latter, which is also the one selected for the future Kuva Space constellation. This satellite pattern can be fully determined through four parameters. T represents the total number of satellites, uniformly distributed in each of the P orbit planes. i is the inclination of the orbits, which is supposed to be the same for all. The last term is F, and is defined as the relative spacing between satellites in adjacent planes. In a constellation $\Delta\phi$ is defined like the *phase difference*, which is the angle in the direction of motion from the ascending node to the nearest satellite at a time when a satellite in the next most westerly plane is at its ascending node. $\Delta\phi$ must be an integral multiple of $360°/T$, and can be any integer number from 0 to $P-1$: this value is F [3].

$$i : T/P/F \tag{2.11}$$

Equation 2.11 shows the shorthand notation used to indicate a Walker Delta constellation. An example of a Walker Delta configuration is displayed in figure 2.4.

2.3.2 Constellation Design

2.4 Orbit Maintenance

Over the life of a space mission, the need to adjust or maintain the orbit elements might arise. In general, orbit maintenance is required because of two main reasons: targeting to reach an end orbit or position (such as a rendezvous maneuver), or to maintain absolute or relative orientations (as for station-keeping) [3].

Figure 2.4: Illustration of a 65:15/3/2 Walker Delta configuration [3].

This thesis studies two different scenarios of orbit management. The first one is the *station-keeping*, which aims at routinely restoring the mission nominal altitude and inclination of the case studies analysed. Secondly, the study of the *orbit phasing* is carried out with the purpose of achieving the desired pattern of a group of satellites along the same orbit.

2.4.1 Station-Keeping

From LEO to geostationary orbit (GEO), station-keeping maneuvers must be considered due to perturbations, if requested by one or more mission requirements. In the case of Earth observation applications, electro-optical sensors and radars are generally designed to work approximately at a specific distance from the ground. In addition, the repetition factor Q introduced in the paragraph 2.2.2 will be significantly altered by even small changes in the semimajor axis. Therefore, focusing on the orbits of interest of this research, perturbations to inclination and SMA must be counteracted if SSO and repeating ground track properties want to be preserved. Moreover, the orbit altitude's maintenance must be taken into account to increase the lifetime of a mission. Indeed, the latter condition is strongly required by the main case study of this thesis.

More in detail, changes in inclination are predominately driven by third body perturbations, whereas variations in the SMA come from atmospheric drag. Both for a single satellite and a constellation mission, each spacecraft has to regularly perform annual Inclination Adjust Maneuvers (IAM) and periodic Drag Make Up (DMU) maneuvers to compensate these perturbing effects, respectively [21]. Note that orbit elements variations under examination are always secular.

In a constellation scenario, station-keeping has the further role of maintaining the desired relative position between satellites, affected by perturbations and variations in the initial conditions for each individual satellite [3].

Spacecraft can rely on on-board propulsive systems to compensate all these disturbances. All the case studies examined in chapter 5 deal with small satellites, which are typically designed without any kind of thrusters or with low-thrust engines. The scenarios of this thesis that involve forces generated by thrusters rely on the *Edelbaum-Kechichian* formulas to obtain realistic simulations.

Edelbaum-Kechichian Theory

An analytic solution for the optimum low-thrust transfer between inclined circular orbits of different radius is provided by the equations of Edelbaum reformulated by Kechichian in 1992 [22, 23]. This thesis takes advantage of this theory to compute ΔV, burning time and related acceleration needed to satisfy the requirements of station-keeping.

The problem assumes only tangential and out-of-plane acceleration, and circular orbits during the transfer ($e = 0$). These assumptions are widely acceptable in this context, because all the case studies of this research are characterized by near-circular orbits, and the thrust direction of the satellites is ideally intended to be parallel to the velocity vector.

The first input parameter is the thrust force acceleration f, deriving from the ratio between the thrust provided by the thruster and the spacecraft mass,

which is broken down into three mutually orthogonal components: the first one is tangential to the velocity vector of the satellite, the second component is normal to the orbital plane, and the last one is normal to the other two. They are expressed in terms of two angles: α is the angle between the velocity vector and the component of the thrust vector in the plane of the orbit, while β represents the angle between the thrust vector and the plane of the orbit [22].

$$f_T = f\cos\beta\cos\alpha \qquad f_N = f\cos\beta\sin\alpha \qquad f_z = f\sin\beta \tag{2.12}$$

Initial and final desired orbit are only assigned by the variations in semimajor axis an inclination (Δa, Δi). From the initial and final semimajor axis, the velocities V_0 and V_f are computed

$$V_0 = \sqrt{\frac{\mu}{a_0}} \qquad V_f = \sqrt{\frac{\mu}{a_f}} \tag{2.13}$$

where μ is always the Earth's gravity constant. Kechichian's reformulation derives the initial angle β_0 from the velocities in 2.13 and Δi:

$$\beta_0 = \tan^{-1}\frac{\sin\frac{\pi}{2}\Delta i}{\frac{V_0}{V_f} - \cos\frac{\pi}{2}\Delta i} \tag{2.14}$$

It is then possible to write the total ΔV

$$\Delta V = V_0\cos\beta_0 - \frac{V_0\sin\beta_0}{\tan\left(\frac{\pi}{2}\Delta i + \beta_0\right)} \tag{2.15}$$

and consequently achieve the transfer time

$$t_f = \frac{\Delta V}{f} \tag{2.16}$$

In case of coplanar transfers, Δi is equal to 0 and ΔV will be simply given by the

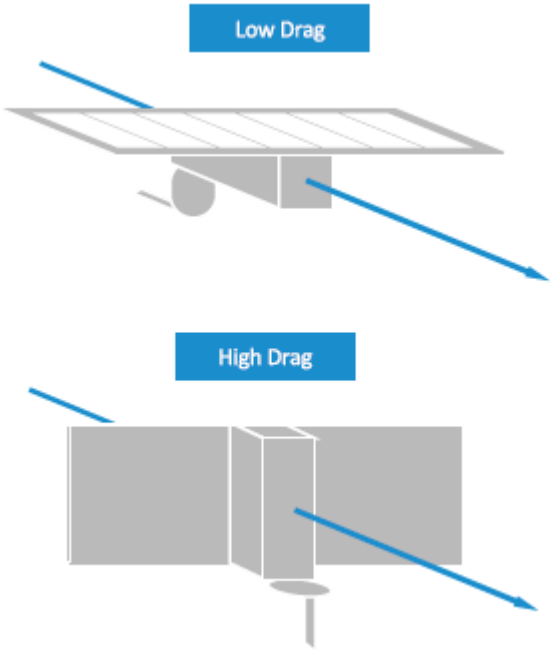

Figure 2.5: Low drag vs. high drag mode example for a simple satellite shape [4].

difference of the velocities in equation 2.13 [23].

2.4.2 Differential Drag Method

Differential drag can be defined as the difference in atmospheric drag acting on each of a couple of satellites. Assuming that the spacecrafts travel through similar atmospheric density areas, the differential drag is almost fully determined by differences in ballistic coefficient of them [24]. Considering identical satellites, and remembering that BC depends on the area perpendicular to the velocity vector, differential drag can be achieved controlling the attitude of the body, leading to different values of surface exposed to the aerodynamic flux.

To clarify ideas and simplify the problem, only two attitudes will be identified as shown in figure 2.5: low drag and high drag modes. Moreover, the satellite on the lower orbit will be indicated as the *leading satellite*, whereas the other one *trailing satellite*. Imagining of using differential drag only to equalize the altitudes, with both spacecrafts travelling in low drag mode, the trailing satellite shall be set

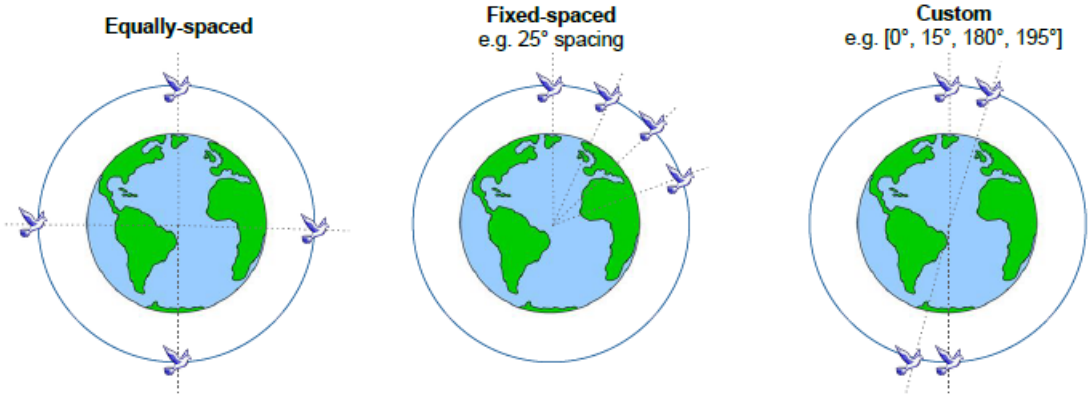

Figure 2.6: Generic cases of desired relative placement of four satellites [4].

to high drag mode until the leader's orbit is reached. Indeed, the acceleration of its motion is the same as if the air drag force, reversed, were pushing the satellite. This phenomena is known as *satellite paradox* [25].

Several applications can take advantage from differential drag. It was first proposed for *formationkeeping* to keep a satellite in a specific position with respect to another. Even rendezvous maneuvers involve differential drag actions for its initial phase. This method has also been selected for collision avoidance scenarios.

What is of huge interest for the purposes of the thesis is the experience provided by Planet company. They applied differential drag control to fleets of propulsion-less satellites deployed in the same orbit with successful results for several missions. The goal of Planet's controller was to bring all the spacecrafts at the same altitude and perform phasing with only differential drag after deployment from launcher. Three examples of constellation phasing are shown in figure 2.6 The initial conditions subsequent to the deployment contain small but significant variations in SMA: achieving the same orbital altitude means zero-relative speed between them. On the other hand, the phasing aims to symmetrically separate the vehicles in terms of angular distance, along the same orbit. Once the desired constellation pattern is achieved, the differential drag control continues to operate as station-keeping to maintain the formation, since the propulsion-less nature of

the satellites.

[4]

2.4.3 Space Debris Mitigation

Chapter 3

Methodology

Exclusively open-source resources have been used to carry out the thesis work. In particular, the orbital scenarios under examination have been simulated through dynamic propagation models created in Python, taking advantage of existing free Python libraries. In order to validate the results, the General Mission Analysis Tool (GMAT) has been chosen as the reference software to make comparisons. In the following paragraphs a brief description of the tools mentioned previously is presented.

3.1 Python for Astrodynamics Applications

Due to the computationally intensive nature of astrodynamics tasks, astrodynamicists have relied on compiled programming languages such as Fortran for the development of astrodynamics software. Interpreted languages like Python on the other hand offer higher flexibility and development speed thereby increasing the productivity of the programmer. While interpreted languages are generally slower than compiled languages, recent developments such as just-in-time (JIT) compilers or transpilers have been able to close this speed gap significantly. Another important factor for the usefulness of a programming language is its wider ecosys-

tem which consists of the available open-source packages and development tools including integrated development environments and debuggers.

In light of the above, Python can be considered as a suitable language for scientific computing due to the existence of well established libraries like NumPy and SciPy for mathematical calculations. Not only do these libraries make use of compiled code from existing accelerated libraries, but it is also possible in Python to interface with compiled code to speed up specific algorithms where required. This allows a user to define a problem in Python, while benefiting from the speed of compiled languages for computationally expensive algorithms. Indeed, JIT-compiled dynamic languages such as Python with Numba have reached a competitive level of performance while still offering the advantages of lower complexity and better programmer productivity [26].

And not for nothing, nowadays, by a wide margin, Python is the most popular interpreted language in astronomy [27].

3.1.1 Numba

Arguably, the most important library in the scientific Python stack is NumPy, which implements n-dimensional arrays and its related methods in C programming language, and wraps them using the CPython API (Application Programming interface). It is a fundamental piece of software that powers most numerical codes written in Python nowadays. However, while it is possible to vectorize certain kinds of numerical operations, there might be other cases where this may not be feasible and where the dynamic nature of Python leads to a performance penalty, especially when the algorithm involves several levels of nested looping. To overcome these limitations it is possible to use Numba, an open-source library which can infer types for array-oriented and math-heavy Python code and generate optimized machine instructions using the LLVM compiler infrastructure [28].

In brief, Numba is a JIT compiler for scientific Python, which allows to optimize the running time.

3.1.2 poliastro

`poliastro` is an open-source Python library for astrodynamics and orbital mechanics released under the MIT (Massachusetts Institute of Technology) license. It features algorithms which are written in pure Python and compiled using Numba. It is dedicated to astrodynamics applications, such as orbit propagation, resolution of the Kepler and Lambert problems, conversion between position and velocity vectors and classical orbital elements and orbit plotting [28]. In addition, thanks to Astropy, poliastro can perform seamless coordinate frame conversions and use proper pysical units and timescales. At the moment, poliastro is the longest-lived Python library for astrodynamics, has contributors from all around the world, and several New Space companies and people in academia use it [29].

3.2 General Mission Analysis Tool

The General Mission Analysis Tool is a software system for trajectory optimization, mission analysis, trajectory estimation, and prediction developed by NASA (National Aeronautics and Space Administration), the Air Force Research Lab, and private industry. GMAT is designed to model, optimize, and estimate spacecraft trajectories in flight regimes ranging from LEO to lunar applications, interplanetary trajectories, and other deep space missions. GMAT's design and implementation are based on four basic principles: open-source visibility for both the source code and design documentation; platform independence; modular design; and user extensibility [30].

3.3 Debris Risk Assessment and Mitigation Analysis

Chapter 4

Satellite Constellation Management Tools

4.1 Orbit Propagators

4.1.1 Undisturbed Motion

4.1.2 Perturbations

4.1.3 Atmospheric Models

4.1.4 Mean Orbital Elements Converter

4.1.5 Sun Synchronous Orbits Functions

4.1.6 Satellite Constellation Propagator

4.2 Revisit Time Collector

4.3 Station-Keeping Simulator

4.4 Differential Drag Algorithm

Chapter 5

Case Studies

5.1 Reaktor Hello World

5.2 Hyperfield Next Generation

5.3 Planet CubeSat Constellation

5.4 Future Kuva Constellation

Chapter 6

Analysis and Results

6.1 Reaktor Hello World Life Data

6.2 Hyperfield Orbit Maintenance Design

6.3 Planet Constellation Differential Drag Results

6.4 Kuva Constellation Management Results

Chapter 7

Conclusion

Donec et nisl id sapien blandit mattis. Aenean dictum odio sit amet risus. Morbi purus. Nulla a est sit amet purus venenatis iaculis. Vivamus viverra purus vel magna. Donec in justo sed odio malesuada dapibus. Nunc ultrices aliquam nunc. Vivamus facilisis pellentesque velit. Nulla nunc velit, vulputate dapibus, vulputate id, mattis ac, justo. Nam mattis elit dapibus purus. Quisque enim risus, congue non, elementum ut, mattis quis, sem. Quisque elit.

Bibliography

[1] Charles D Brown. *Spacecraft mission design*. AIAA, 1998.

[2] Howard D Curtis. *Orbital Mechanics for Engineering Students: Revised Reprint*. Butterworth-Heinemann, 2020.

[3] James R Wertz. Orbit & constellation design & management, 2nd printing. *Hawthorne, CA and NY: Microcosm Press and Springer*, 2009.

[4] Cyrus Foster, James Mason, Vivek Vittaldev, Lawrence Leung, Vincent Beukelaers, Leon Stepan, and Rob Zimmerman. Differential drag control scheme for large constellation of planet satellites and on-orbit results. *arXiv preprint arXiv:1806.01218*, 2018.

[5] Craig A Kluever. *Space flight dynamics*. John Wiley & Sons, 2018.

[6] Michael Douglas Griffin. *Space vehicle design*. AIAA, 2004.

[7] David A. Vallado. *Fundamentals of Astrodynamics and Applications*. Microcosm Press, fourth edition, 2013.

[8] Ian Ridpath. *A dictionary of astronomy*. Oxford Quick Reference, 2012.

[9] Kathleen Riesing. Orbit determination from two line element sets of iss-deployed cubesats. 2015.

[10] Mohammad Sadraey and Dr Müller. Drag force and drag coefficient. *M. Sadraey, Aircraft Performance Analysis. VDM Verlag Dr. Müller*, 2009.

[11] Bruce R Bowman, W Kent Tobiska, Frank A Marcos, and Cesar Valladares. The jb2006 empirical thermospheric density model. *Journal of Atmospheric and Solar-Terrestrial Physics*, 70(5):774–793, 2008.

[12] Bruce Bowman, W Kent Tobiska, Frank Marcos, Cheryl Huang, Chin Lin, and William Burke. A new empirical thermospheric density model jb2008 using new solar and geomagnetic indices. In *AIAA/AAS astrodynamics specialist conference and exhibit*, page 6438, 2008.

[13] Giorgio EO Giacaglia. Long-period perturbations in the inclination of sun-synchronous satellites. *Revista Brasileira de Ciencias Mecanicas (ISSN 0100-7386*, 16:583–589, 1994.

[14] HG Walter. Conversion of osculating orbital elements into mean elements. *The Astronomical Journal*, 72:994, 1967.

[15] Gim J Der and Roy Danchick. Conversion of osculating orbital elements to mean orbital elements. In *Flight Mechanics/Estimation Theory Symposium 1996*, 1996.

[16] David Arnas. Analytic transformation from osculating to mean elements under j2 perturbation. *arXiv preprint arXiv:2212.08746*, 2022.

[17] Hanspeter Schaub and John L. Junkins. *Analytical Mechanics of Aerospace Systems*. 2002.

[18] Ronald J Boain. Ab-cs of sun-synchronous orbit mission design. 2004.

[19] Xin Luo, Maocai Wang, Guangming Dai, Xiaoyu Chen, et al. A novel technique to compute the revisit time of satellites and its application in remote sensing satellite optimization design. *International Journal of Aerospace Engineering*, 2017, 2017.

[20] Lloyd Wood. Satellite constellation networks: The path from orbital geometry through network topology to autonomous systems. *Internetworking and computing over satellite networks*, pages 13–34, 2003.

[21] Megan R Johnson and Jeremy D Petersen. Maintaining aura's orbit requirements while performing orbit maintenance maneuvers containing an orbit normal delta-v component. In *International Symposium on Space Flight Dynamics*, number GSFC-E-DAA-TN14128, 2014.

[22] Theodore N Edelbaum. Propulsion requirements for controllable satellites. *Ars Journal*, 31(8):1079–1089, 1961.

[23] J KECHICHIAN. The reformulation of edelbaum's low-thrust transfer problem using optimal control theory. In *Astrodynamics Conference*, page 4576, 1992.

[24] Carolina Lee Leonard. *Formationkeeping of spacecraft via differential drag*. PhD thesis, Massachusetts Institute of Technology, 1991.

[25] Blake D Mills. Satellite paradox. *American Journal of Physics*, 27(2):115–117, 1959.

[26] Helge Eichhorn, Juan Luis Cano, Frazer McLean, and Reiner Anderl. A comparative study of programming languages for next-generation astrodynamics systems. *CEAS Space Journal*, 10:115–123, 2018.

[27] Ivelina Momcheva and Erik Tollerud. Software use in astronomy: an informal survey. *arXiv preprint arXiv:1507.03989*, 2015.

[28] Juan Luis Cano Rodríguez, Helge Eichhorn, and Frazer McLean. Poliastro: an astrodynamics library written in python with fortran performance. In *6th International Conference on Astrodynamics Tools and Techniques*, 2016.

[29] Juan Luis Cano Rodríguez and Jorge Martínez Garrido. poliastro: a python library for interactive astrodynamics. 2022.

[30] Darrel J Conway and Steven P Hughes. The general mission analysis tool (gmat): Current features and adding custom functionality. In *International Conference on Astrodynamics Tools and Techniques (ICATT)*, number LEGNEW-OLDGSFC-GSFC-LN-1107, 2010.